Flying qualities reliability constraints in aircraft conceptual design using time-marching simulations

Marco Saporito * and Andrea Da Ronch †
Engineering and Physical Sciences, University of Southampton, Southampton SO17 1BJ, UK

Nathalie Bartoli ‡ and Sébastien Defoort §
ONERA/DTIS, Université de Toulouse, F–31055 Toulouse, France

Aircraft conceptual design, especially when novel concepts are involved, is inherently affected by uncertainty. Although many efforts are done to include more physics at the earliest design phases, often information on impact of the underlying uncertainty is missing. This work proposes an approach to incorporate uncertainty into aircraft conceptual design through reliability constraints on some desired dynamic performance requirements. These are estimated from unsteady time-domain simulations through a system identification process, leveraging on three available aerodynamic fidelity levels. Uncertainty propagation is addressed by a polynomial chaos expansion technique. After presenting the structure and the validation of the proposed framework, a demonstrative application of fuel mass optimization for a transport aircraft under uncertainty is performed, with reliability constraints on short period characteristics.

I. Introduction

AIRCRAFT design is complex and multifaceted. The traditional design process has been developed assuming a weak interaction among disciplines. The design was optimised for each discipline in turn, treated like "silos" [1]. This approach started to show signs of inadequacy with the advent of new lightweight materials and the trends to increase the wing span, in a continued search for better performance. More recently, there has been a large body of work focusing on the development of a concurrent design process, embedded within a multi–disciplinary analysis and optimisation framework [2–5]. Whilst successful in their attempts to further improve the aircraft performance, these modern approaches are often carried out at the detailed phase of the design process. As a result, the number of parameters describing the disciplinary models (external aerodynamic shape, internal structural elements, etc.) is very high, and certainly incompatible with feasibility and exploratory studies. To this goal, we aim at developing an aircraft sizing process to support decision making at the early phases of the design process, scouting multiple and radically different vehicle concepts. Unique to our approach is the ability to include aleatory and epistemic uncertainties, ranging from design parameters (manufacturing), operating conditions (sensed information) to numerical schemes (mathematical models), into design considerations, and leverage on this information to identify aircraft designs that meet reliability constraints.

To this end, the present work proposes a framework to address the following tasks: 1) predict some desired key performance indices on the aircraft dynamic stability in support of conceptual design evaluations, where conventional and unconventional configurations can be analysed by selecting the appropriate fidelity levels among those available; 2) estimate, based on an uncertainty quantification study, the reliability of the calculated figures of merit when uncertain input parameters are present; 3) provide the information on the dynamic performance and the related uncertainty to an aircraft sizing and optimization tool to enable a reliability constrained optimization study.

More in details, although the developed modules allow a certain generality in the problem definition, spanning from purely aerodynamic characterization, to longitudinal, lateral and directional stability or control sensitiveness, the study here presented concerns aircraft longitudinal dynamic stability. The effort is to extend the use of classic stability specification constraints, such as those on linear damping ratios or frequencies, to cases where the classical analytical

*PhD student. Email: m.saporito@soton.ac.uk
†Associate professor. AIAA Senior Member. Email: a.da-ronch@soton.ac.uk
‡Senior researcher, Information Processing and Systems Department. AIAA Member. Email: nathalie.bartoli@onera.fr
§Head of Multidisciplinary Methods and Integrated Concepts Group, Information Processing and Systems Department. Email: sebastien.defoort@onera.fr

computation of those parameters is not a trivial task and more advanced strategies are required. In future work, this will be applied to cases including structural dynamic behaviour modelling.

This paper initially describes the implementation of the framework and its modules, and their validation against conventional test-cases. Then, an application on a reliability-constrained optimization problem based on the proposed methodology is demonstrated. The paper continues in Section II with a discussion of the available computational tools. Some of them have already been presented in the literature, whereas others have been developed or introduced only recently to enhance the capabilities of the framework. For the latter case, some validation studies are reported in Section III. Section IV presents an application to a fuel mass optimization for a transport aircraft with respect to planform parameters, under longitudinal flying qualities reliability constraints. Uncertainty is considered to arise from the estimation of mass distribution, and is therefore associated to the center of gravity (CG) location and to the moment of inertia of the vehicle. Conclusions are then given in Section V.

II. Formulation

The computational framework builds upon the `FAST-OAD` aircraft sizing tool (standing for Future Aircraft Sizing Tool - Overall Aircraft Design) [6]. The open source software* has been developed by ONERA and ISAE-SUPAERO since 2015 and it is conceived as a quick conceptual design tool for tube and wing configurations. The user specifies a series of Top Level Requirements and the framework computes the aircraft geometry and estimates the required fuel consumption through a series of sizing loops involving modular analyses for the key disciplines, namely flight mechanics, aerodynamics, structures, propulsion, weight and balance. The original approach is based on a point mass approximation together with semi–empirical equations for performance and aerodynamic predictions. This allows high computational efficiency and accuracy to be achieved as long as traditional concepts are treated. The propulsion module can be based either on a dataset from the CeRAS project [7], or on an analytical model that provides thrust and fuel consumption as function of altitude and flight speed [8]. The performance module gathers all the information from the disciplinary modules and performs a time marching simulation of the full mission. Sizing and positioning of components are iteratively updated during the design loops through dedicated geometry, weight and balance modules. Overall aircraft design rules from [9] are used to initially locate the main components, such as wing, tail, landing gear, etc. `FAST-OAD` has recently been enhanced by embedding physics–based analysis tools to extend its applicability to novel aircraft concept [10].

This work extends the platform with a toolset dedicated to the analysis of dynamic performances of the sized airplane, allowing for uncertainty to be propagated onto the desired figures of merit. The toolkit takes as input the information about lifting surfaces configuration, flight conditions, weight and balance, thrust. It is composed by the following modules:

- A choice of aerodynamic models, including a classical analytical model based on linear aerodynamic derivatives, and a steady or unsteady implementation of the Vortex Lattice Method (VLM/UVLM);
- A flight dynamics simulation module (FDM) implementing the 6DOFs non-linear equations of motion;
- A post-processing module that extracts amplitude, frequency and damping information out of the simulation history by use of a fitting technique of the time-domain data;
- An Uncertainty Quantification (UQ) and sensitivity analysis module that wraps the above modules and propagates the uncertainty from the input parameters into the desired quantity of interest (QoI). It returns the required statistical metrics to be used in the reliability evaluation.
- A Bayesian optimization toolbox, whose advantage is the capability to handle black-box optimization tasks exploiting Gaussian processes to speed up expensive computations.

The framework allows addressing at least three possible optimization problems: 1) a reliability-constrained optimization where a figure of merit (such as fuel) is minimized under a stochastic constraint based on the probability of matching a certain performance (such as the generic damping ξ); 2) a robust optimization where the expectation of a certain target (such as fuel) is minimized against some uncertain input variables; 3) a combination of the two. In this work the framework is applied to a case study of the first type. The global architecture is summarized in Fig. 1. The optimizer requires to define the optimization variables, their bounds, the constraints and the objective function. In this case the optimization variables are denoted as V_g. For each candidate evaluation the uncertainty quantification module takes into account the prescribed distributions of the uncertain parameters and runs an adequate number of calls to the multidisciplinary analysis (MDA) in order to compute the statistical metrics associated to one or more QoIs. In the present study the chosen metrics are the 5% and 95% percentiles of the short period damping and natural

*`https://github.com/fast-aircraft-design/FAST-OAD`

frequency, indicated as $P5\left(\xi_{sp}, \omega_{n\,sp}\right)$ and $P95\left(\xi_{sp}, \omega_{n\,sp}\right)$. These values are compared by the optimizer with the required boundaries to enforce the reliability constraints. The MDA starts with the `FAST-OAD` sizing process, which receives the design variables V_g and returns a converged configuration characterized by additional geometric parameters P_g, an estimation of the CG location x_{CG}, and other indicators such as the mission fuel mass, which is here used as objective function. The configuration returned by `FAST-OAD` is subsequently given to the UVLM module, with a CG position altered by Δx_{CG}, representing its uncertainty. The unsteady solver simulates some pitching oscillations at the frequency ω_0, which is assumed a representative short period frequency for the particular class of aircraft considered. The time response in terms of aerodynamic loads is then processed to extrapolate an equivalent, derivative-based aerodynamic model characterized by a set of coefficients C_{L_i}, C_{L_i} (defined later in Section II.A). The assumption here is that even if each candidate has a slightly different frequency, this variation adds a negligible aerodynamic contribution compared to the model obtained at ω_0. The assumption is reasonable because, given the relatively high flight speed, a small variation of ω produces a negligible variation of the reduced frequency $k = \omega\,\bar{c}/2\,V$, which is the parameter that really affects the unsteady aerodynamics. Once the aerodynamic derivatives are identified, they are fed to the flight dynamics module, together with the other aircraft parameters P_g and the longitudinal moment of inertia I_{yy}, given by the uncertainty quantification module. Here the time response (in this case the longitudinal short period response) is computed following a disturbance, and the time domain results are then processed to get the desired QoI, in this case the short period damping ξ_{sp} and natural frequency $\omega_{n\,\text{sp}}$. More details on the single disciplinary modules mentioned above are given in the following sections.

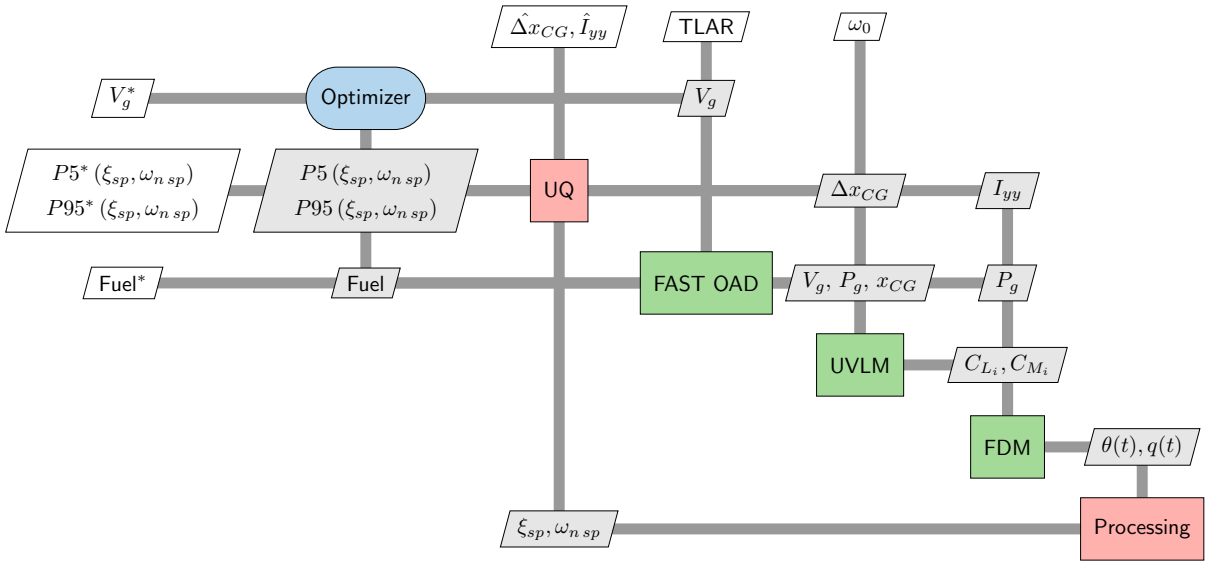

Fig. 1 Framework for aircraft multidisciplinary design and optimization under reliability constraints. The diagram is built according to the graphical XDSM structure proposed in [11].

A. Aerodynamic Models

The quest for an appropriate mathematical model of aerodynamic loads for flight simulation is a long–standing challenge. A multitude of approaches has been proposed [1, 12, 13], but the challenge still remains: how to retain unsteady and nonlinear flow effects for applications requiring fast turn–around times, such as in conceptual design? Herein, we leverage on three possible options.

The first and simplest method is the canonical form based on Bryan's approach [14], where the six aerodynamic coefficients are linearly dependent on the state variables through a series of aerodynamic derivatives:

$$\begin{aligned} &C_i = C_{i_\alpha} \cdot \alpha + C_{i_\beta} \cdot \beta + C_{i_V} \cdot V + C_{i_q p} \cdot p + C_{i_q} \cdot q + \ldots \\ &\text{with} \quad C_i = C_L, C_Y, C_D, C_m, C_l, C_r \end{aligned} \tag{1}$$

The aerodynamic terms in Eq. (1) need to be computed or measured. Within this work, the VLM is used to calculate these terms. An alternative is to run the VLM in a standalone manner, so that aerodynamic forces and moments are directly exchanged to the FDM module once relevant input parameters are known (speed, aerodynamic angles, angular rates, etc.). The VLM implementation follows that of Katz and Plotkin [15]. The assumptions are of potential, incompressible flow around zero–thickness lifting surfaces, an approach generally recognised as adequate for early evaluations, and compatible with the restricted set of geometrical parameters available at this stage. For more complex studies, which may involve for example high frequency oscillations, control design, gust or aeroelastic coupling, the unsteady version of the VLM (UVLM) can be employed. The main difference is in that a more complex wake model is used, where at each time step a new row of wake panels is shed from the trailing edge, and each wake panel is convected along the direction of the local flow speed. In this way a more accurate evaluation of the three-dimensional flow interaction is achieved, and the information on the past history is kept to influence the present flow conditions.

As the aerodynamic module is often the most computationally expensive in aeronautics, again the Fortran language was preferred instead of more comfortable but less efficient interpreted languages. The Fortran modules, namely the flight dynamics and the VLM/UVLM modules, are then wrapped to be called within the remaining high-level routines, all of which are coded in Python. The wrapping is done in two steps: a) first, a static library is created containing the full Fortran project, b) then a small list of routines to be exposed via Python are wrapped by use of the `f90wrap` [16] utility and compiled together with the static library into the final product, a dynamic library that can be imported in Python to access the desired Fortran routines.

The verification of VLM module and its coupling with the flight dynamics simulation module are briefly presented in Section III.A.

B. Flight dynamics module

A flight dynamics simulation module was developed to support the design process with the possibility of visualizing the vehicle behaviour under desired flight conditions. In order to be adaptable to a wide variety of configurations, the architecture is retained simple and easy to interface. Also, the formulation is kept as general as possible, and the full 6DOFs non-linear equations of motion have no simplifying assumptions other than that of flat, non-rotating earth. The aerodynamic loads can be imported as an external function, so that the module is independent on the aerodynamic formulation. Any of the three aerodynamic modules presented in this work can be called according to the particular necessities of the examined case. Mass and inertia are allowed to vary, and no assumptions are made on the vehicle symmetry. The equations of motion are integrated using second and third order numerical schemes. The software was coded in a compiled language (Fortran) to ensure a high execution speed. When a precomputed aerodynamic database is employed one simulation of around 10 seconds flight is run in a small fraction of second, a speed comparable to other analysis methods such as linear eigenvalue analysis or other frequency domain techniques. Stability analysis and modal characteristics can still be achieved via the processing module that will be introduced in Section II.C. A validation study for this module is briefly described in Section III.B.

C. System Identification

The primary scope of a simulation tool as the one described above is to quickly visualize the time domain performance of the candidate vehicle with higher fidelity approaches with respect to those commonly available at conceptual design level, based on analytical and semi-empirical relationships tailored on well-known conventional architectures. The aim is to capture the major aerodynamic interactions in unconventional geometries and related control surface layouts (such as for strut-braced wings, box-wings, asymmetric geometries), possible non-linear rigid body effects as those described in Section III.A or flight dynamics and aeroelastic interactions. This, of course, should come compatibly with the low level of detail available and with the requirements of affordable computational time. To accomplish this, this work leverages on some parameter identification techniques that exploit the higher–fidelity time simulation data to extrapolate desired QoIs. Here this strategy is applied at two levels. On one hand an identification technique extrapolates a reduced order aerodynamic model from unsteady time domain UVLM simulations. The process identifies a set of aerodynamic derivatives that form a quasi–steady model capable to reproduce with good approximation the UVLM results. This process is detailed in Section II.C.1. On the other hand, a second technique is applied to the flight simulation results to identify the main modal characteristics of the response. This is done here to determine the short period damping and frequency, but the approach is general and could be applied in future applications to filter other information, such as lateral modes, structural stress or aeroelastic modes. The approach is described in Section II.C.2.

1. Unsteady aerodynamic derivatives

The derivation of a quasi–steady aerodynamic model follows the approach described in [17]. First, the unsteady solution has to be obtained with a high-fidelity solver (the UVLM in this case) for a forced oscillating motion. Enough oscillation cycles must be run in order to let the transient response vanish, achieving the periodic evolution. This could take two or three cycles at high frequency, but in the present case it was found that the transient decays in a small fraction of a period. Once the periodic evolution of the aerodynamic coefficients is available, the derivatives can be identified by assuming a law of the type:

$$\Delta C_i = C_{i\alpha}\,\Delta\alpha + C_{iq}\left(\frac{\bar{c}}{2V}\right) q + C_{i\dot{\alpha}}\left(\frac{\bar{c}}{2V}\right)\dot{\alpha} + C_{i\ddot{\alpha}}\left(\frac{\bar{c}}{2V}\right)^2 \ddot{\alpha} \qquad (i = D, L, m) \tag{2}$$

For a sinusoidal pitch oscillation with $\alpha(t) = \alpha_0 \sin(\omega t)$ the aerodynamic variables of interest are:

$$\dot{\alpha} = q = \alpha_0\,\omega\,\cos(\omega t) \tag{3}$$

$$\ddot{\alpha} = \dot{q} = -\alpha_0\,\omega^2\,\sin(\omega t) \tag{4}$$

Equation (2) then becomes:

$$\Delta C_i = \bar{C}_{i\alpha}\,\alpha_0\,\sin(\omega t) + \bar{C}_{iq}\,\alpha_0\,\cos(\omega t) \tag{5}$$

with:

$$\bar{C}_{i\alpha} = (C_{i\alpha} - k^2\,C_{i\ddot{\alpha}}) \tag{6}$$

$$\bar{C}_{iq} = (C_{iq} + C_{i\dot{\alpha}}) \tag{7}$$

where $k = \omega\,\bar{c}/(2V)$ is the reduced frequency. Equation (5) represents a truncated Fourier series for $C_i(wt)$, and therefore the coefficients (6) and (7) can be obtained as:

$$\bar{C}_{i\alpha} = \frac{2}{\alpha_0\,n\,T}\int_0^{nT} \Delta C_i(t)\,\sin(\omega t)\,dt \tag{8}$$

$$\bar{C}_{iq} = \frac{2}{\alpha_0\,k\,n\,T}\int_0^{nT} \Delta C_i(t)\,\cos(\omega t)\,dt \tag{9}$$

These coefficients were computed by numerical integration of the $C_L(t)$ and $C_M(t)$ curves obtained with the UVLM. The $C_{i\alpha}$ and C_{iq} coefficients were computed with the steady VLM. Ultimately, with these quantities known, the remaining terms $C_{i\dot{\alpha}}$ and $C_{i\ddot{\alpha}}$ where obtained from (6) and (7). The approach is demonstrated in Fig. 2, where the lift and moment coefficients obtained with the steady and unsteady derivatives are compared with the output curves from the UVLM. It can be seen that the linear model based on the identified unsteady derivatives matches satisfactorily the reference curve, except for the initial transient due to the start of motion. An appreciable difference is found with respect to the prediction based on static derivatives only.

2. Flying qualities

Although the time domain visualization of the aircraft response under a higher fidelity representation is already an added value in support of the decision making, the effort here is to further exploit the simulation data to be used within an automatic process of performance characterization within feasibility and optimization studies. In particular, it is still interesting at this design stage to have access to quantifiable figures of merit, such as frequencies or damping ratios, that are typical of linear system analysis. The estimation of such parameters would enable to assess the compliance with dynamic specification constraints, which are mostly about linear system characterization, even for design concepts that are not well represented, or at least not *a priori*, by the conventional, knowledge-based, linear characterization. Moreover, a linear Jacobian of a complex, non-linear coupled system, such as for flexible airplanes dynamics, may not always be available, depending on the models employed and how their coupling is implemented. For this reason, an effort is done here to process the time domain simulation data and extrapolate a set of figures of merit - corresponding

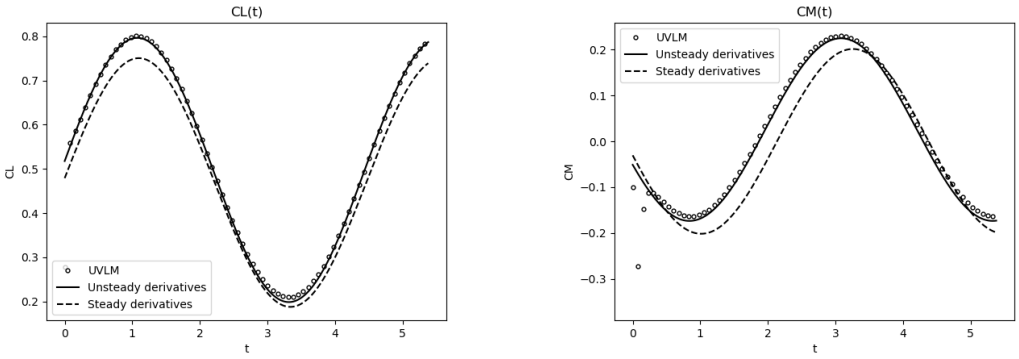

(a) Lift coefficient **(b) Moment coefficient**

Fig. 2 Identification of lift coefficient time history under forced pitch oscillations.

to linear damping and frequency - that with the best approximation describe the obtained non-linear response. It should be noted that when assigning some linear descriptors (frequency, damping) to a non-linear curve, an approximation is inevitably demanded. The advantage here is that such approximation is done *a posteriori* based on the full non-linear results, and its adequacy can be verified against those.

To this purpose, different signal processing techniques have been tested, including Dynamic Mode Decomposition (DMD) [18], Empirical Modal Decomposition (EMD) [19], the Hilbert Transform[†], useful to extract damping ratios, the Fast Fourier Transform (FFT)[‡], the Prony method [20] and some Least Squares fitting techniques[§]. The method to be used shall be selected according to the complexity of the problem. For example, two-dimensional aeroelastic simulations, or constrained flight dynamics simulations - such as those used in Section III.A - are expected to show simpler dynamic characteristics compared to 3D aeroelastic or full 6DOFs coupled manoeuvres.

When the objective of the processing module is to extrapolate frequencies and damping ratios, the Prony method was found effective and robust enough. It performs a curve fitting similar to the Fast Fourier Transform, returning a best fit function of complex exponential form:

$$\tilde{F}(t) = \sum_{i=1}^{N} A_i \, e^{\lambda_i t} \tag{10}$$

where $A_i$and λ_i are both complex coefficients, and N the number of vibration modes to retain. This can be either estimated by an FFT analysis, or fixed by the user if a certain behaviour is expected. For the initial testing of the presented framework, the category of problems investigated can be adequately described by just one or two modes, simplifying the fitting process. For example, Fig. 3 reports the curve fitting of some random 4th-order harmonic oscillations combining both converging and diverging modes. In this case, the Prony fitting of Eq. (10) with $N = 4$ perfectly captured the dynamics identifying the two dominant frequencies and damping ratios.

D. Uncertainty Quantification

As mentioned above, early aircraft analysis is inherently affected by uncertainty, both of aleatory and epistemic kind. In this work, which focuses on aircraft flying qualities estimation at conceptual design level, we aim at including and propagating the most relevant uncertainties onto the desired output performance indicators. More in details, this work restricts the investigation into longitudinal dynamics, and therefore the uncertainty herein considered is that arising from the approximate methods used during the sizing process to estimate weight and balance characteristics. In this case, typical uncertain parameters would be the location of the center of gravity, the moment of inertia, the relative position and orientation between main and stabilizing lifting surfaces. In this preliminary development stage, the off-the-shelf `Uncertainpy` toolbox [21] was chosen for uncertainty quantification and sensitivity analysis and interfaced with the performance analysis modules. The toolbox, originally conceived mainly for computational neuroscience, is easily

[†] `Scipy.signal.hilbert`, `https://docs.scipy.org/doc/scipy/reference/generated/scipy.signal.hilbert.html`

[‡] `Scipy.fft`, `https://docs.scipy.org/doc/scipy/reference/tutorial/fft.html`

[§] `Scipy.optimize.curve_fit`, `https://docs.scipy.org/doc/scipy/reference/generated/scipy.optimize.curve_fit.html`

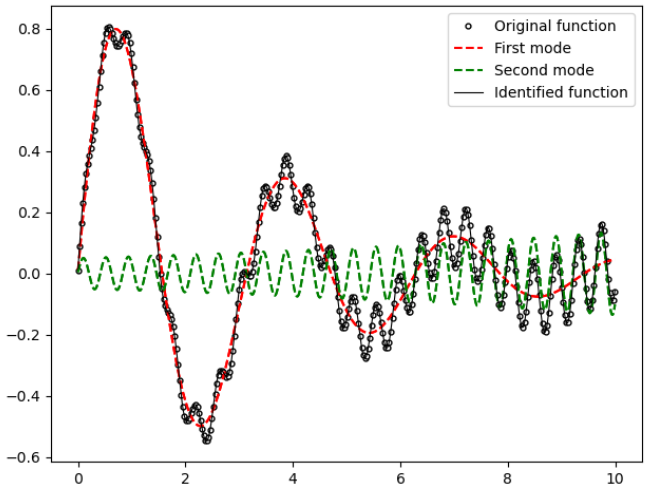

Fig. 3 Example curve fitting of a 4th-order oscillator function via the Prony method.

adaptable to any computational field in that it is a model-independent, open source, Python-based platform. The main features of the platform are here briefly summarized. The sensitivity analysis is addressed by computation of first-order Sobol indices and total Sobol indices when interactions between the uncertain parameters exist. As far as uncertainty quantification is concerned, it implements both quasi-Monte Carlo methods and Polynomial Chaos Expansions (PCE) using non-intrusive methods. The quasi-Monte Carlo methods employ variance-reduction techniques to reduce the number of model evaluations needed. As for the PCE approach, the orthogonal polynomials are found using the three-term recurrence relation, and the expansion coefficients can be found either through the Tikhonov regularization, belonging to the class of point collocation methods, or by a pseudo-spectral approach based on Leja quadrature and Smolyak sparse grids. The Sobol first and total order methods can be computed directly from the PCE [22]. The output metrics provided are the QoI mean, variance, 5% and 95% percentiles and the Sobol indices. Additionally, some modifications were made to obtain the Probability Distribution Function (PDF) together with any desired percentile. Before using the framework for aerospace-related applications, the UQ module was tested and validated against a benchmark case to prove its effectiveness. The validation is presented Section III.C.

E. Surrogate modelling

The work here presented leverages on the use of effective and well-proven surrogate modelling techniques to speed-up the analyses involving the most expensive disciplines. To this purpose, the python open-source `SMT`[¶] toolbox was adopted [23]. The tool provides several customizable options for surrogate modelling, including Kriging, Radial Basis Functions, Least Squares approximations, among others. For the applications reported in this work, a Kriging approach based on constant regression trend and Gaussian correlation function was adopted as it gave satisfactory performances. In all cases the Design of Experiments was built via a Latin Hypercube Sampling algorithm, also available from `SMT`.

F. Bayesian Optimization

The optimization task performed in this work relies on a Bayesian Optimization approach using the `SEGOMOE` toolbox (standing for Super Efficient Global Optimization with Mixture of Experts) by ONERA and ISAE-SUPAERO [24]. The advantage of Bayesian optimization is that no derivative needs to be computed through finite differences, and therefore the required number of function calls is considerably reduced compared to other approaches. Moreover, the method leverages on Gaussian surrogate modelling of the objective function and constraints, enhanced by different available adaptive learning strategies. In this work the enrichment process was guided by the Watson and Barnes

[¶] `https://github.com/SMTorg/smt`

criterion (WB2) [25] that gives slightly more merit to local search. Constraints were handled by means of Upper Trust Bound [26], which encourages exploration of the feasible domain by combining the mean prediction and the associated uncertainty function given by the Gaussian processes. Two optimization algorithms to solve the subproblem related to the acquisition function were tested: COBYLA and SLSQP, both associated to a multistart approach to achieve global search. The latter was adopted as it has proven more stable for this specific case.

III. Verification of the added tools

A. Aerodynamics

As one target application of the present framework is a transport aircraft design and optimization task, a validation study is here reported to show the good match of the developed VLM module against available data and models regarding the A320-like CeRAS baseline. A first reference is the CeRAS database itself. A second reference, here denoted as L0, is the aerodynamic model already validated and embedded into the `FAST-OAD` tool, based on semi–empirical relations only. To make sure that the VLM can be interfaced consistently with the framework, a hybrid aerodynamic model was built, named L1, where trim and induced drag are taken from the VLM, whereas viscous and compressibility drag are the same as for L0. The VLM representation of the CeRAS baseline is shown in Fig. 4a. The comparison of the drag polars from L0, L1 and the CeRAS database is reported in Fig. 4b, showing that the VLM-based model is quite close to the reference data.

A validation on another test case of the present unsteady VLM formulation is now presented. The verification is done by comparison with the unsteady theory of Theodorsen [27]. In this case, as the theory concerns two-dimensional flow around thin airfoils, a single wing with a very high aspect ratio ($\mathcal{R}$= 100) was used in the 3D UVLM model. Three frequencies were employed from $k = 0.25$ up to $k = 0.75$, a value which is far high with respect to those generally expected for wings and aerodynamic actuators during airplane operations. A good matching was obtained as shown in Fig. 5.

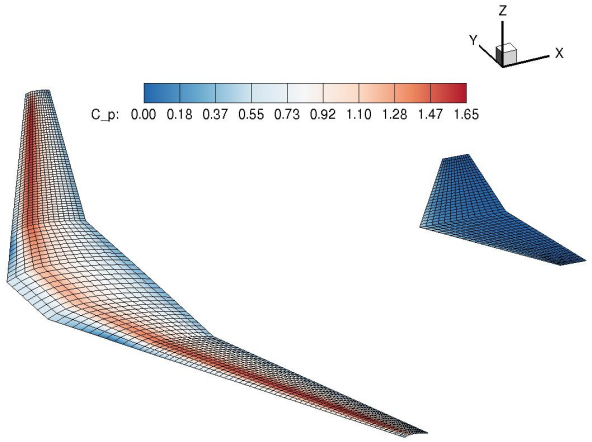

(a) VLM representation

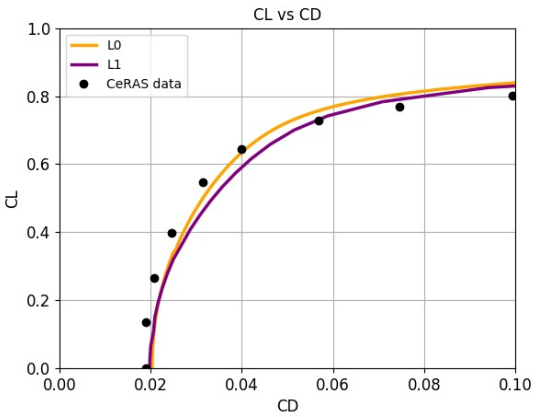

(b) Cruise drag polars

Fig. 4 Application of the present VLM tool to the `FAST-OAD` platform. (a) VLM representation of the A320 baseline. (b) Comparison of the A320-baseline cruise drag polars computed with the `FAST-OAD` semi-empirical aerodynamic model (L0) and with an adapted version of the present VLM (L1). Data from the CeRAS [7] database are also reported for validation.

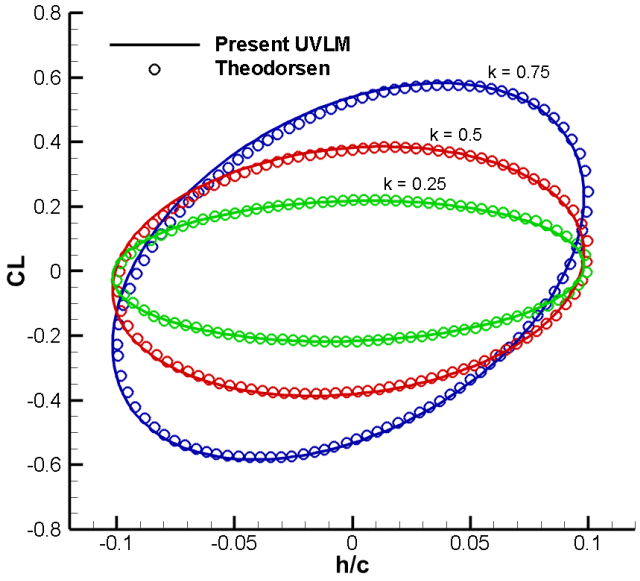

Fig. 5 Validation of the UVLM solver. Lift coefficient of a 2D thin profile in harmonic plunging oscillations, for three reduced frequencies. Comparison against the theoretical model of Theodorsen [27], data from [28].

B. Flight dynamics

The test case is for a small manoeuvrable airplane performing a fast rotational motion. The reference simulation data are from [29], and the aircraft parameters can be found in [30], including the aerodynamic derivatives provided for a linear description of the vehicle aerodynamics. The simulation reproduces a fully coupled manoeuvre where the non–linearities of the equations of motion become relevant. Two cases are reported corresponding to aileron deflections of $\delta_a = -4.0^\circ$ and $\delta_a = -5.0^\circ$. In both cases, a pitch–down initial condition is imposed by setting the elevator to $\delta_e = 2.0^\circ$. The time history of the angles of attack and sideslip are reported in Fig. 6. The test case shows that a small difference in the control input causes the response to diverge within a couple of seconds from the equilibrium point. The unstable oscillations experienced when the aileron deflection is $\delta_a = -5.0^\circ$ are exclusively due to the nonlinear inertial coupling of the equations of motion. A dynamic model linearized around the same stable initial condition would not be able to predict such a behaviour, and would give instead stable oscillations around the initial equilibrium as those corresponding to $\delta_e = -4^\circ$, where the rotational rates are not sufficiently large to make the system lose its stability.

C. Uncertainty quantification

A benchmark mathematical problem was chosen from the literature to verify the `Uncertainpy` results. The example is adopted from [31] where an uncertainty quantification using dimensional adaptive polynomial chaos expansion was performed on the following function:

$$g(x_1, x_2, x_3) = 0.25 \left(\sin(x_1 - 3)(x_2 - 1) + (x_3 - 1)^2\right) - 1 \tag{11}$$

with uncertainty on the three input variables as described in Tab. 1.

The `Uncertainpy` PCE was used with the point collocation method. The resulting PDF after 72 model evaluations is compared with that from [31] in Fig. 7. Also, a comparison is reported in Tab. 2, based on the available data from the reference, on the quantile $\bar{q}$ which is predicted to satisfy a certain probability threshold $\bar{P}$. Other methods are used in the reference paper: first-order reliability methods (FORM), second-order reliability methods (SORM) and the probability density evolution method (PDEM). For these methods the values of $\bar{q}$ are not given, and in this case only the number of evaluations needed to complete the UQ task is available and reported in the table for comparison. The validation shows that the adopted method performs well and with good efficiency compared with other methods.

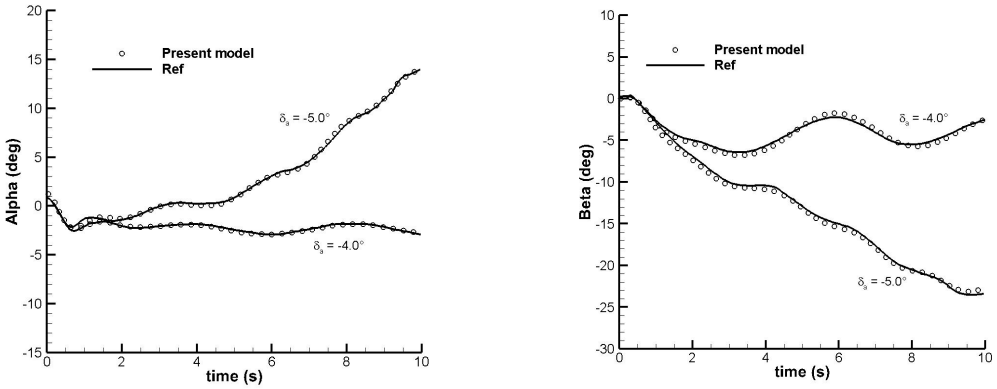

(a) Angle of attack. **(b) Sideslip angle.**

Fig. 6 Validation of the non-linear 6-DOFs flight dynamics simulation module. Reference data from [29].

Variable	Distribution	Range
x_1	Uniform	[0.0 , 10.0]
x_2	Uniform	[6.0 , 16.0]
x_3	Uniform	[0.0 , 10.0]

Table 1 Uncertain ranges and distributions of variables for the test-case in Eq. (11)**.**

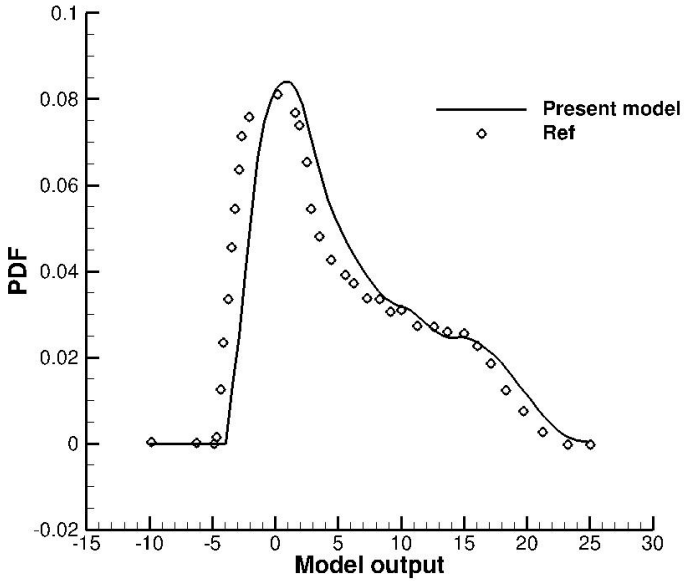

Fig. 7 Comparison of the PDF obtained with the present approach against data from [31].

IV. Application: transport aircraft planform optimization under uncertainty

A first application of the discussed framework is here presented. The case study aims at optimizing the planform of an A320-like configuration with respect to the fuel mass required for a representative flight, under reliability constraints

	$\bar{q}$ s.t. $P\{q(X)\} > \bar{P}$			
Method	$\bar{\mathbf{P}}$ = **28.4**%	$\bar{\mathbf{P}}$ = **77.4**%	$\bar{\mathbf{P}}$ = **99.3**%	**Evaluations**
Monte Carlo [31]	~ 0.5	~ 10.0	~ 20.0	10^6
Dimensional Adaptive PCE [31]	0.0	10.0	20.0	11
`Uncertainpy`	1.1	10.9	21.2	73
FORM [31]	-	-	-	96
SORM [31]	-	-	-	123
PDEM [31]	-	-	-	135

Table 2 Comparison of output metrics from the UQ module for the validation test-case.

on the short period dynamics. The reference configuration is the CeRAS baseline (see Fig. 8), whose main characteristics are summarized in Tab. 3. Four geometric parameters were chosen as optimization variables: the taper ratio and the quarter-chord sweep of the main wing and horizontal tail. Although previous studies [10] showed that aspect ratio may play a key role in fuel mass optimization, it was decided here not to include it among the optimization variables. In fact, highly elongated wings would require further aeroelastic verification, which is not available at the current state of the presented framework. It was assumed instead that the baseline aspect ratio is already the best trade-off between aerodynamic efficiency and structural mass. The chosen variables and their bounds are summarized in Tab. 4. Uncertainty is associated to the estimation of the center of gravity location x_{CG} and to the longitudinal moment of inertia I_{yy}. The propagation of this uncertainty through the MDA is handled by the uncertainty quantification module, which ultimately returns the probabilities of constraints violations. Four flying qualities constraints were applied: the upper and lower bounds of short period damping ξ_{sp} and natural frequency $\omega_{n\,\text{sp}}$. This choice arises from the fact that short period characteristics in particular have critical influence on manoeuvrability. Of course this study does not aim at a complete treatment of flying qualities requirements, which would require a prohibitive effort for the collection and codification of the certification specifications. Instead, we want to present a proof of concept of the proposed framework, showing the capability to handle multidisciplinary aircraft design and optimization under uncertainty, with reliability constraints on aerodynamic and/or dynamic performances. Which performance constraints to enforce will be a case-dependent choice of each particular study.

Fig. 8 CeRAS baseline planform, from [32].

Top Level Aircraft Requirements	
Number of passengers	150
Passenger weight [lbs]	200
Design Range [NM]	2750
Operational Range [NM]	800
Cruise Mach number	0.78
Approach speed [kts]	132
Planform parameters	
Wing area [m^2]	122.4
Mean aerodynamic chord (MAC) [m]	4.2
Aspect ratio	9.48
Wing break	0.40
Wing sweep angle at 25% chord [deg]	24.5
Wing taper ratio	0.313
Horizontal tail sweep angle at 25% chord [deg]	28.0
Horizontal tail taper ratio	0.300
Propulsion	
Max thrust at sea level [N]	117880
Weight & balance	
Max take-off weight [N]	7.55×10^5
Selected nominal CG location	45%MAC
Pitching moment of inertia [kg$\times m^2$]	3.6×10^6

Table 3 CeRAS baseline parameters, from [32].

Design variables	**Symbol**	**Lower bound**	**Upper bound**
Main wing taper ratio	$t_{r\,W}$	0.25	0.37
Main wing sweep at 25% chord	Λ_W	20°	29°
Horizontal tail taper ratio	$t_{r\,T}$	0.24	0.36
Horizontal tail sweep at 25% chord	Λ_T	23°	34°

Table 4 Design Variables and relative boundaries.

A. Aerodynamics and flight dynamics

The unsteady aerodynamics module based on the UVLM (see Section II.A) and the derivatives identification techniques of Section II.C.1 are here employed to compute the full set of derivatives needed for longitudinal flight simulation. A snapshot from a UVLM simulation of the CeRAS baseline is reported in Fig. 9. These simulations impose a sinusoidal pitching oscillation and return the time history of the force and moment coefficients. As the short period is not really affected by drag, only lift and moment coefficients are taken into account. The imposed pitching motion is of the form:

$$\alpha(t) = \alpha_M + \alpha_0 \sin(\omega t) \tag{12}$$

with $\alpha_M = 5.0°$ and $\alpha_0 = 3.0°$. The choice of oscillations around a non-zero angle of attack is mainly due to the fact that it is of no interest to include negative angles of attack for an airliner configuration. It is preferable instead to span a larger portion of the positive, linear range of angles of attack. An example of the lift and moment responses is reported in Fig. 10. It can be seen that the unsteady aerodynamics capture two main differences with respect to the steady model. The first is an amplitude gap, especially visible in the lift coefficient curve, producing a higher lift for the unsteady case. This translates into a slightly steeper slope of the $C_L - \alpha$ ellipse. The second effect, mainly affecting the pitching

moment, is a phase anticipation of the unsteady moment with respect to the steady one. That appears clearly in the time-domain curve and it is even more evident from the larger $C_L - \alpha$ ellipse. These effects are to be attributed to the interaction between main wing and tail, and in particular to tail downwash delay, whose effect is to let the main wing lift coefficient grow bigger and the main wing moment coefficient to grow earlier than the steady prediction, where the tail effect is considered immediate.

The aerodynamic calculations were carried out around a trimmed climb configuration with $\alpha = \theta = \alpha_M$, where θ_b is the pitch angle. The trim is achieved by a Newton algorithm to find the nonlinear equilibrium with the steady VLM. The nonlinearity comes from the fact that a change in the tail tilt angle also changes loads and loads distribution, so that an iterative process is required to achieve balance. The UVLM is then run from the trimmed geometry. This allows to be consistent with the following flight dynamics simulation, which is then started from an equilibrium condition at $\alpha = \alpha_M$. The flight dynamics module, taking as input the configuration file including the computed derivatives, returns the response to a step pitch control. The output is then processed as described in Section II.C.2 to extract the damping and frequency of the short period mode.

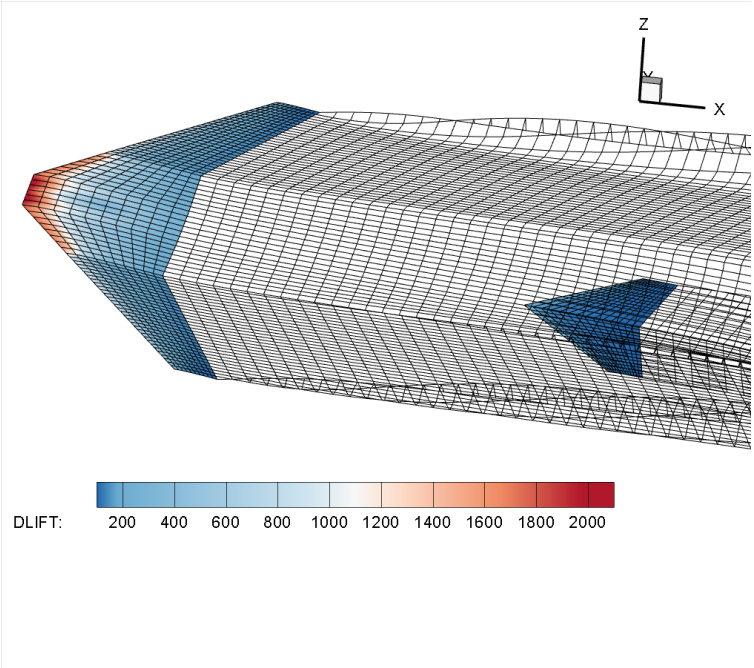

Fig. 9 Snapshot during unsteady simulation of the CeRAS A320 baseline, run with the present UVLM solver.

B. Surrogate modelling of the aircraft sizing process and aerodynamic characterization

The aircraft sizing process and the aerodynamic characterization of the converged configuration are the most expensive tasks in the present MDAO chain. Running the optimization and uncertainty quantification loops with the full architecture showed in Fig. 1 would reach prohibitive costs for conceptual exploration and design (the study presented herein would require several days as one single run of the UVLM analysis takes around on our). For this reason it was chosen to build a surrogate model of sizing and aerodynamic characterization of the design candidates. The `FAST-OAD` output depends only on the geometrical optimization variables V_g. The UVLM solver requires as input, in addition to V_g, a complementary set of geometrical outputs from `FAST-OAD`, P_{g1} (root chords, distance between main wing and tail, nominal center of gravity location, etc) and the uncertainty on the center of gravity location Δx_{CG}, and its ultimate output, after the derivative identification process, is the set of aerodynamic derivatives to be fed to the flight dynamics module. Therefore the block `FAST-OAD`+UVLM takes five inputs (the four optimization variables V_g plus the uncertain parameter Δx_{CG}) and outputs the fuel mass objective function, the eight aerodynamic derivatives (C_{L_α}, C_{L_q},$C_{L_{\dot\alpha}}$,$C_{L_{\ddot\alpha}}$,C_{M_α}, C_{M_q},$C_{M_{\dot\alpha}}$,$C_{M_{\ddot\alpha}}$) and the remaining aircraft parameters P_{g2} needed by the flight dynamics module (wing area and mean aerodynamic chord). Overall, the block takes five inputs and returns ten outputs. The structure of this updated version of the MDAO framework is summarized in Fig. 11. A Gaussian process was chosen as surrogate

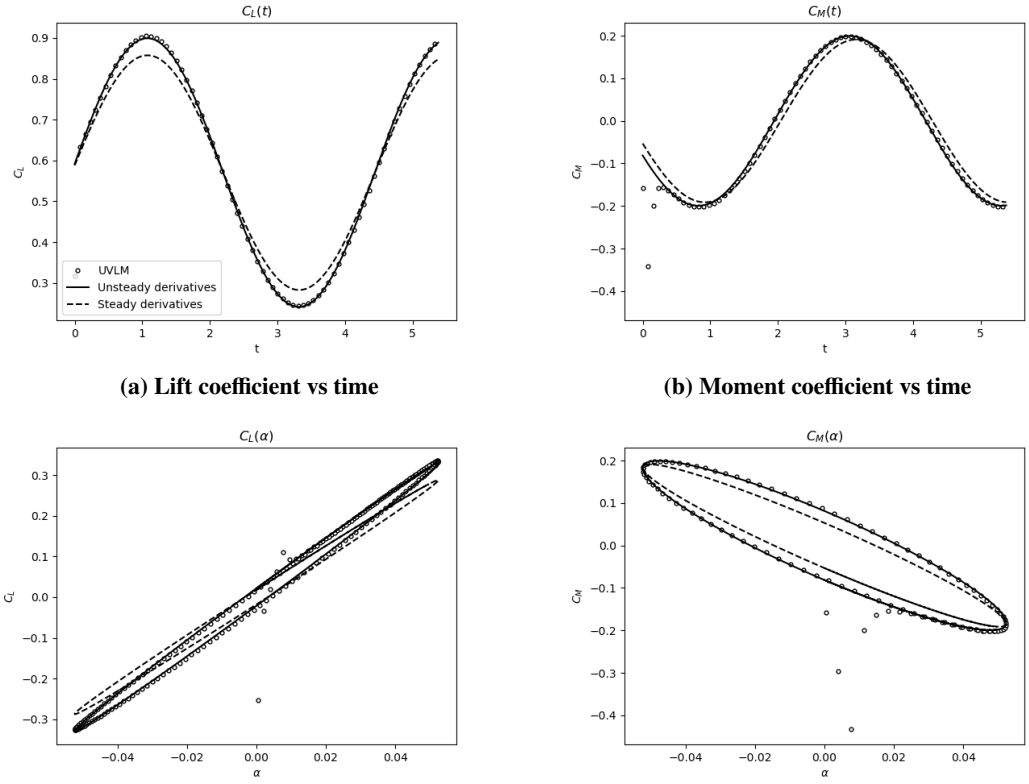

(a) Lift coefficient vs time

(b) Moment coefficient vs time

(c) Lift coefficient vs angle of attack

(d) Moment coefficient vs angle of attack

Fig. 10 Example of aerodynamic responses to pitch oscillations and their identification via linear derivatives.

model. This generally requires around $10\times N_{\text{dim}}$ sample points to reach adequate precision. As in this case $N_{\text{dim}} = 5$, a DOE of 65 samples was set up via Latin Hypercube Sampling, accounting for about 20% extra points to be used for validation. The training points and the test points were selected through the `ScikitLearn` toolbox [33]. With this set up the surrogate model gave satisfactory results for all the outputs, with a root mean square error always below the 0.3%. The validation is reported in Appendix A.

C. Reliability constraints

As mentioned above, the dynamic constraints here adopted are on the short period damping and natural frequency. A wide set of possibilities is available from the literature for flying qualities specifications or recommendations, including qualitative and quantitative guidance, in frequency and time domain. In this work the quantitative definition of the constraints was made starting from the so-called longitudinal short period *thumb print* criterion. It defines some regions in the $\xi_{\text{sp}} - \omega_{n\,\text{sp}}$ plane corresponding to different pilot ratings such as satisfactory, acceptable, poor, unacceptable. The diagram is reported in Fig. 12. The figure also shows four lines defining the scalar values adopted here as upper and lower bounds for the two parameters. It is worth pointing out that as ξ_{sp} is expected to stay close to the lower bound, the upper bound on $\omega_{n\,\text{sp}}$ was fixed close to the satisfactory limit corresponding to $\xi_{\text{sp, min}}$. The values for each bound is given in Tab. 6.

With these scalar bounds fixed, the reliability problem is based on the probability of those bounds to be violated: acceptable configurations are considered those for which the probability to fall within the bounds is greater than 95%. Before running the optimization task, the capability of the uncertainty quantification module to well predict the statistics for the quantities of interest was tested with a single, random combination of the design variables V_g. An uncertainty quantification with the PCE method introduced in Section II.D was run on this configuration assigning the following uncertainty distributions reported in Tab. 5. The choice of these different distributions is due to the fact that `FAST-OAD` gives an estimation for the CG location but not for the moment of inertia. The results were validated against a distribution

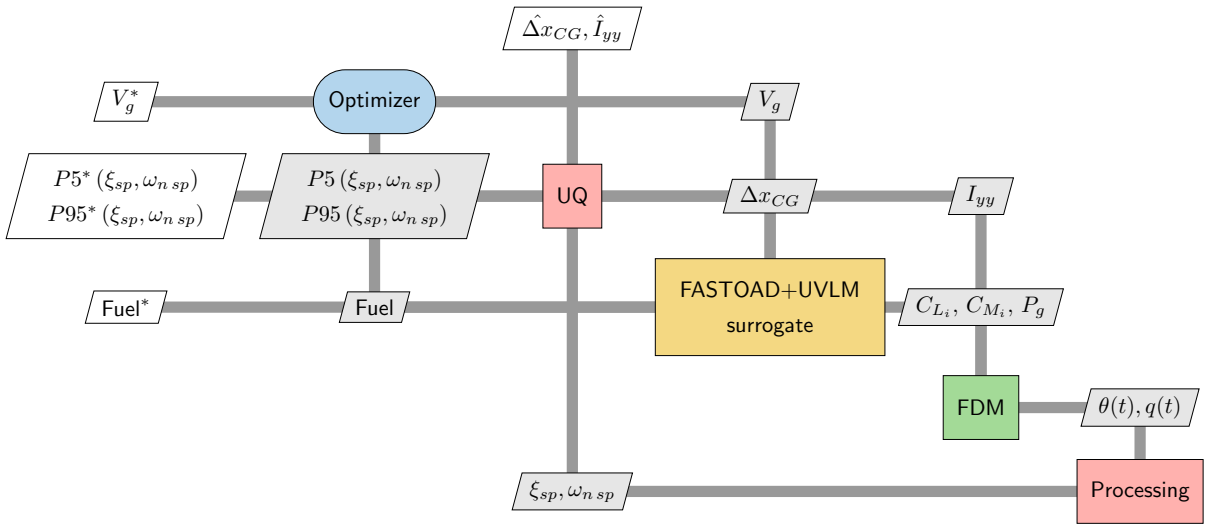

Fig. 11 Framework for robust design and optimization under reliability constraints. Shaded fields are susceptible to uncertainty.

obtained via a Monte Carlo simulation with 10^4 samples. A probability distribution function was extrapolated from the PCE evaluating it at 10^5 samples, and this is compared in Figs. 13a and 13b with a histogram chart built from the Monte Carlo results. The outcome demonstrated that the PCE approach is able to reproduce the model with satisfactory accuracy. It was found that a polynomial order of 4, using point collocation method and the Hammersley sampling with 32 function calls was sufficient as no appreciable improvement was obtained by increasing the order up to 6 and the function calls up to 80. The main statistical metrics are reported in Figs. 13c and 13d. It also confirms that the sensitivity analysis is consistent as the first Sobol indices correctly sum to 1. It is worth pointing out that the obtained distributions are wide enough to approach the constraint boundaries of Tab. 6, which justifies the search for optimal constrained configuration.

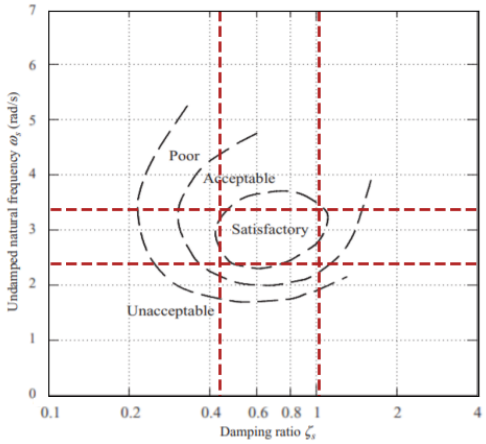

Fig. 12 Thumb print criterion reporting the pilot opinion contours related to the short period characteristics. The dashed red lines show the bounds used in this work.

Parameter	Distribution	Descriptors
Δx_{CG}	Normal	$\mu = \bar{x}_{CG}, \quad \sigma^2 = 0.1\,\bar{x}_{CG}$
I_{yy}	Uniform	$I_{\min} = 0.8\,I_{yyB}, \quad I_{\max} = 1.2\,I_{yyB}$

Table 5 Uncertainty distributions on the input parameters. $\bar{x}_{CG}$ is the CG location for a prescribed load case defined in `FAST-OAD`. I_{yyB} is the moment of inertia of the baseline configuration.

Parameter	Lower bound	Upper bound
ξ_{sp}	0.45	1.35
$\omega_{n\,\text{sp}}$	2.4	3.4

Table 6 Short period damping and natural frequency constraints adopted for the present case study.

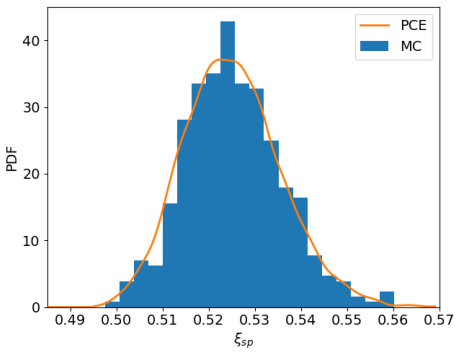

(a) Short period damping - PDF

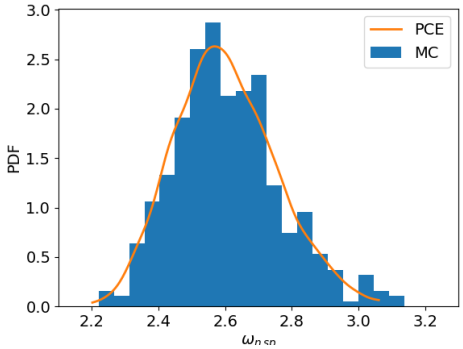

(b) Short period natural frequency - PDF

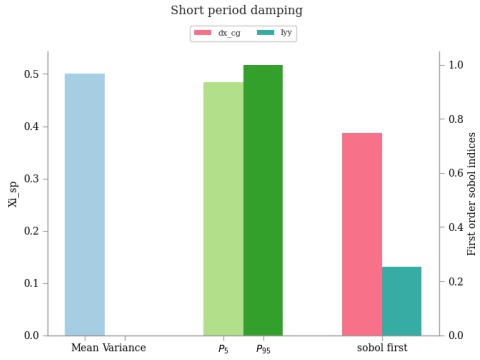

(c) Short period damping - statistical metrics

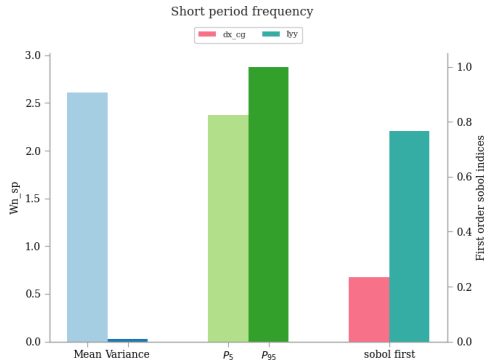

(d) Short period frequency - statistical metrics

Fig. 13 Validation of the PCE approach for a reference configuration ($t_{r\,W} = 0.3$, $\Lambda_W = 25°$, $t_{r\,T} = 0.28$, , $\Lambda_T = 28°$).

D. Optimization results

The overall optimization task is summarized in Tab 7. In order to perform the optimization with the `SEGOMOE` tool it is required to define a learning DOE, which is used to build a Gaussian process for the black-box function to optimize. A DOE size of 60 points was given, and additional 100 calls were allowed to the optimizer as exploration iterations. At each iteration, the optimizer updates the surrogate with the added knowledge and maximizes the WB2 acquisition function to choose the next candidate to evaluate. The learning and optimization history is reported in Fig. 14. It can be seen that the optimizer rapidly converges to candidates very close to the optimum in few iterations after running the

DOE, demonstrating that the learning was sufficient to identify the most promising design regions. The 100 iterations were also enough to explore the design space, as no relevant changes in the objective function were found after the first iterations. In a few cases the expected improvement moved towards worse candidates, sometimes giving a very high value of the objective function. It was found that the best configurations in terms of fuel burn always have satisfactory short period characteristics with respect to the given constraints. In particular, the only constraint which is sometimes violated is the lower bound on natural frequency, whereas the others are matched in all cases. This could be explained by recalling, from classical notions of flight dynamics [30, 34] that a low short period frequency could arise mainly from a low absolute value of the aerodynamic stiffness in pitch C_{M_α} (the sign is always negative), or from a high moment of inertia, or both. As the inertia is here distributed in the same way for every configuration, the correlation between higher fuel consumption and lower short period frequency is to be found on the aerodynamic pitch stiffness. In effect, the module of C_{M_α} is reduced with a backward shift of the CG but also with a lower slope C_{L_α}, and the latter decreases with a decrease on efficiency. Moreover, a very low pitch stiffness due to wing shape is automatically compensated in the sizing process with a more effective (larger) tail plane, which translates into a heavier and consequently less efficient configuration. For this reasons the most aerodynamically efficient configurations also provide good short period characteristics, and conversely the worst shapes promoting inefficient load distributions also determine a deterioration of the short period response. It is also interesting to note, from Fig. 15, that low sweep angles Λ_W never comply with the constraints. The reason is linked with the above discussion: low sweep angles have here the effect of moving the aerodynamic center forward, reducing the static margin and the absolute value of the pitch stiffness C_{M_α}, producing lower short period frequencies.

	Function/variable	**Range/distribution**
Minimize	Fuel mass	
with respect to	Main wing taper ratio	[0.25, 0.37]
	Main wing sweep at 25% chord	[20° , 29°]
	Horizontal tail taper ratio	[0.24, 0.36]
	Horizontal tail sweep at 25% chord	[23° , 34°]
with uncertainty on	Center of gravity location	Normal ($\mu = \bar{x}_{CG}$, $\sigma^2 = 0.1\,\bar{x}_{CG}$)
	Longitudinal moment of inertia	Uniform [$0.8\,I_{yy}$, $1.2\,I_{yy}$]
subject to	Prob[ξ_{sp} > 0.45] > 95%	
	Prob[ξ_{sp} < 1.35] > 95%	
	Prob[$\omega_{n\,\text{sp}} > 2.4$] > 95%	
	Prob[$\omega_{n\,\text{sp}} < 3.4$] > 95%	

Table 7 Definition of the optimization problem.

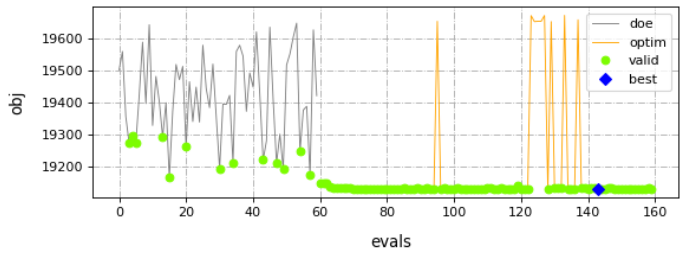

Fig. 14 Monitor plot of the DOE runs and optimization history.

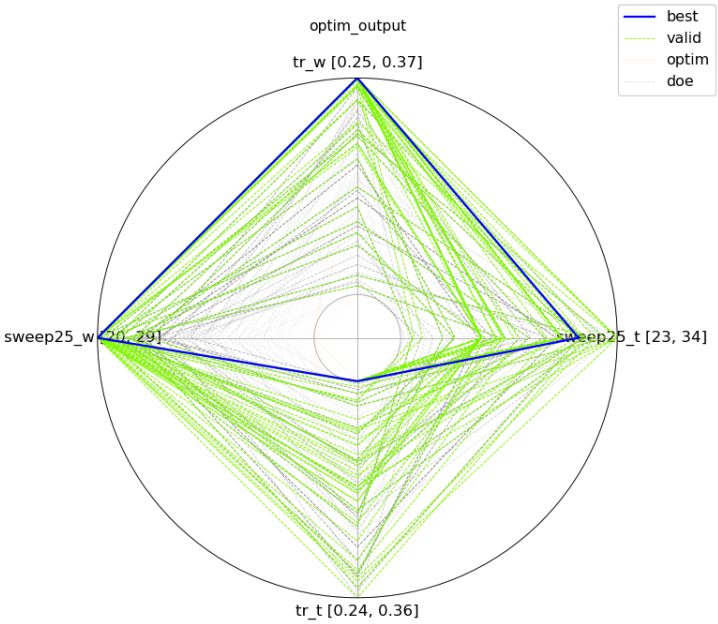

Fig. 15 Radar plot summarizing all the evaluations during the DOE and the optimization iterations.

Source	$t_{r\,W}$	Λ_W	$t_{r\,T}$	Λ_T	Fuel mass (surrogate)	Fuel mass (true)
CeRAS	0.31	24.5°	0.3	28.0°	-	19406 kg
Optimizer	0.37	29.0°	0.24	32.0°	19131 kg	19137 kg

Table 8 Fuel mass optimization results compared with baseline data. The optimized configuration offers an improvement of 1.4%.

V. Conclusions

This work introduced a MDAO framework for aircraft design applications capable to deal with optimization under uncertainty. The framework is composed by a combination of existing tools for aircraft sizing, optimization and uncertainty quantification, and some more recent tools for aerodynamic and flight performance analysis developed, validated and assembled during a PhD project promoted by the University of Southampton, UK, and the ONERA center of Toulouse, FR. First, all the building blocks of the chain have been presented singularly, together with the validation of those tools that have been developed by the author during the PhD project. All of these tools showed good performance for applications involving flight dynamics, system identification, different aerodynamic fidelity levels, including steady and unsteady three-dimensional flow. These tools were proved effective both for stand-alone applications and for coupled analysis. Then, the whole framework was tested on a first case study: a transport aircraft fuel mass optimization with respect to planform variables, with uncertainty on the center of gravity location and on the longitudinal moment of inertia, and under reliability constraints on the short period damping and natural frequency. The unsteady aerodynamics module was used to run a series of oscillating simulations, which were processed to identify a set of aerodynamic derivatives. These were used to set up a much faster aerodynamic function to be called by the flight dynamics module. This enabled a very fast computation of the dynamic response of the aircraft, which can then be processed to get the desired figures of merit, in this case the short period damping and natural frequency. This process is automatically handled by the uncertainty quantification module, that computes the stochastic output, given the distributions of the uncertain input parameters. Such outputs are ultimately passed to the optimizer, which verifies the reliability of the candidate against the required boundaries. The bayesian optimization converged to an optimum satisfying all the given constraints. It was found that the most stringent constraint is the lower bound on the natural frequency, but for the type of vehicle considered all the best candidates in terms of fuel burn also comply with the present short period requirements.

The reason for this was recognized to be the fact that aerodynamic efficiency also translates into increased aerodynamic pitch stiffness, and this relationship is favourable at least for the category of aircraft studied herein.

The framework proved capable to successfully address the multidisciplinary optimization task, with an architecture conceived to be flexible with respect to the problem. In fact, although a reduced set of variables and constraints was here adopted, the same approach and tools are applicable to more complex problems, with increased number of variables or constraints or uncertain parameters. The same kind of analysis could be performed for example to include robust control design, provided that the aerodynamic function is enriched with the needed control laws. In that case more stringent constraints could be applied, and additional dynamic responses could be studied, including lateral dynamics or the complete coupled set of the equations of motion. Moreover, as the aerodynamic tools here presented have already been coupled with a structural dynamic solver of aeroelastic calculations, it is planned to extend the framework to include aeroelastic constraints. This would allow to extend the exploration to larger aspect ratios and more efficient and innovative configurations. Further work will also include a deeper analysis of the model uncertainties introduced by modelling choices and surrogate approaches, to better understand the trade-off between computational time and accuracy for this kind of multidisciplinary reliability analysis.

A. Appendix: verification of the surrogate modelling approach.

The verification of the surrogate model for the aircraft sizing and unsteady aerodynamic calculation processes is here reported. The model depends on 5 variables (the 4 geometric optimization variables V_g plus the error on the CG location Δx_{CG}) and returns 8 aerodynamic derivatives plus 2 aircraft parameters (wing reference area and MAC) and the objective function (fuel mass). Figure 16 shows that all the predicted outputs are in good agreement with the training points, used to train the Gaussian process, and with the test points, excluded from the training and used only for verification. The RMS error was always below 0.3%.

References

[1] Bocola, F., Muscarello, V., Quaranta, G., and Masarati, P., "Pilot In The Loop Aeroservoelastic Simulation in Support to the Conceptual Design of a Fly By Wire Airplane," *AIAA Atmospheric Flight Mechanics Conference, 22-26 June, Dallas,TX*, , No. AIAA 2015-2557, 2015. https://doi.org/10.2514/6.2015-2557.

[2] Rizzi, A., "Modeling & Simulating Aircraft Stability & Control - SimSAC Project," 2010. https://doi.org/10.2514/6.2010-8238, URL https://arc.aiaa.org/doi/abs/10.2514/6.2010-8238.

[3] Trifari, V., Ruocco, M., Cusati, V., Nicolosi, F., and De Marco, A., "MULTI-DISCIPLINARY ANALYSIS AND OPTIMIZATION JAVA TOOL FOR AIRCRAFT DESIGN," 2018.

[4] Cai, Y., Chakraborty, I., and Mavris, D. N., "Integrated Assessment of Vehicle-level Performance of Novel Aircraft Concepts and Subsystem Architectures in Early Design," *New Technologies and Aircraft System Architectures, AIAA Aerospace Sciences Meeting, 8-12 January 2018, Kissimmee, Florida*, , No. AIAA paper 2018-1741, 2018. https://doi.org/10.2514/6.2018-1741, URL https://arc.aiaa.org/doi/abs/10.2514/6.2018-1741.

[5] Bendarkar, M. V., Behere, A., Briceno, S. I., and Mavris, D. N., "A Bayesian Safety Assessment Methodology for Novel Aircraft Architectures and Technologies Using Continuous FHA," , No. AIAA paper 2019-3123, 2019. https://doi.org/10.2514/6.2019-3123, URL https://arc.aiaa.org/doi/abs/10.2514/6.2019-3123.

[6] David, C., Delbecq, S., Defoort, S., Schmollgruber, P., Benard, E., and Pommier-Budinger, V., "From FAST to FAST-OAD: An open source framework for rapid Overall Aircraft Design," *IOP Conference Series: Materials Science and Engineering*, Vol. 1024, No. 1, 2021, p. 012062. https://doi.org/10.1088/1757-899x/1024/1/012062, URL https://doi.org/10.1088/1757-899x/1024/1/012062.

[7] "Central Reference Aircraft Data System," *[on line database]*, 2015. URL https://ceras.ilr.rwth-aachen.de.

[8] Roux, E., "Pour un Approche Analytique de la Dinamique du Vol," *PhD Thesis, ISAESUPAERO, Toulouse.*, 2005.

[9] Dupont W. P., C. C., "Preliminary design of commercial transport aircraft," *Didactic material, ISAESupaero, Toulouse, France*, 2012.

[10] Saporito, M., da Ronch, A., Schmollgruber, P., and Bartoli, N., "Framework development for robust design of novel aircraft concept," *3AF Aerospace Europe Conference, Feb 2020, BOR-DEAUX, France. hal-02904365*, 2020.

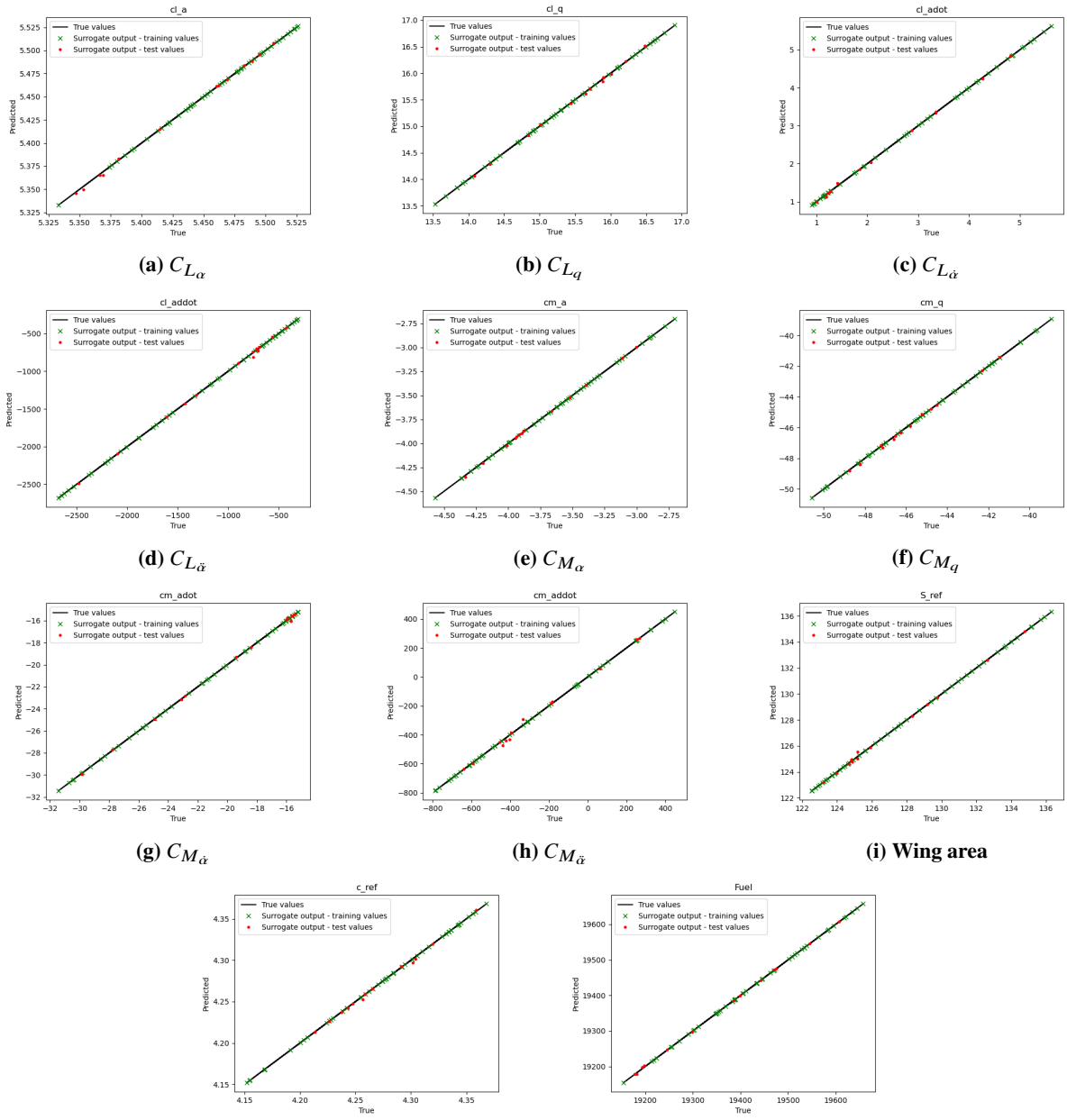

(a) C_{L_α} **(b)** C_{L_q} **(c)** $C_{L_{\dot{\alpha}}}$

(d) $C_{L_{\ddot{\alpha}}}$ **(e)** C_{M_α} **(f)** C_{M_q}

(g) $C_{M_{\dot{\alpha}}}$ **(h)** $C_{M_{\ddot{\alpha}}}$ **(i) Wing area**

(j) Mean aerodynamic chord **(k) Fuel mass**

Fig. 16 Validation of the surrogate models.

[11] Lambe, A. B., and Martins, J. R., "Extensions to the design structure matrix for the description of multidisciplinary design, analysis, and optimization processes," *Structural and Multidisciplinary Optimization, Springer*, Vol. 46, No. 2, 2012, pp. 273–284.

[12] Kharlamov, D., Drofelnik, J., Da Ronch, A., and Walker, S., "Rapid load calculations using an efficient unsteady aerodynamic solver," *AIAA AVIATION Forum, 25-29 June, Atlanta, Georgia, USA*, , No. AIAA paper 2018-3621, 2018. https://doi.org/doi: 10.2514/6.2018-3621, URL https://doi.org/10.2514/6.2018-3621.

[13] Paulino, J. A., Da Ronch, A., Guimarães Neto, A. B., Silvestre, F. J., and Morales, M. A. V., "On real-time simulation of flexible aircraft with physics-based models," *31st Congress of the International Council of the Aeronautical Sciences (ICAS), 09-14 September, Belo Horizonte, Brazil*, , No. 2018-501, 2018.

[14] Bryan, G. H., *Stability in aviation: an introduction to dynamical stability as applied to the motions of aeroplanes*, Macmillan and Company, limited, London, 1911.

[15] Katz, J., and Plotkin, A., *Low-Speed Aerodynamics, Second Edition*, Cambridge University Press, 2001.

[16] Kermode, J. R., "f90wrap: an automated tool for constructing deep Python interfaces to modern Fortran codes," *J. Phys. Condens. Matter*, 2020. https://doi.org/10.1088/1361-648X/ab82d2.

[17] Klein, V., Murphy, P. C., Curry, T. J., and Brandon, J., "Analysis of Wind Tunnel Longitudinal Static and Oscillatory Data of the F-16XL Aircraf," *NASA TM–97–206276*, December, 1997.

[18] Schmid, P. J., "Dynamic mode decomposition of numerical and experimental data," *Journal of fluid mechanics, Cambridge University Press*, Vol. 656, 2010, pp. 5–28.

[19] Laszuk, D., "Python implementation of Empirical Mode Decomposition algorithm," *GitHub Repository*, 2017. URL https://github.com/laszukdawid/PyEMD.

[20] Lobos, T., Rezmer, J., and Schegner, J., "Parameter estimation of distorted signals using Prony method," *2003 IEEE Bologna Power Tech Conference Proceedings,*, Vol. 4, 2003, pp. 5–pp. https://doi.org/10.1109/PTC.2003.1304801, URL https://ieeexplore.ieee.org/abstract/document/1304801.

[21] "Uncertainpy: A Python Toolbox for Uncertainty Quantification and Sensitivity Analysis in Computational Neuroscience," *Front. Neuroinform*, 2018, pp. 12–49. https://doi.org/10.3389/fninf.2018.00049.

[22] Sudret, B., "Global sensitivity analysis using polynomial chaos expansions," *Reliability engineering & system safety*, Vol. 93, No. 7, 2008, pp. 964–979.

[23] Bouhlel, M. A., Hwang, J. T., Bartoli, N., Lafage, R., Morlier, J., and Martins, J. R. R. A., "A Python surrogate modeling framework with derivatives," *Advances in Engineering Software*, 2019, p. 102662. https://doi.org/https://doi.org/10.1016/j.advengsoft.2019.03.005.

[24] Bartoli, N., Lefebvre, T., Dubreuil, S., Olivanti, R., Priem, R., Bons, N., Martins, J. R., and Morlier, J., "Adaptive modeling strategy for constrained global optimization with application to aerodynamic wing design," *Aerospace Science and technology*, Vol. 90, 2019, pp. 85–102.

[25] Watson, A. G., and Barnes, R. J., "Infill sampling criteria to locate extremes," *Mathematical Geology*, Vol. 27, No. 5, 1995, pp. 589–608.

[26] Priem, R., Bartoli, N., Diouane, Y., and Sgueglia, A., "Upper trust bound feasibility criterion for mixed constrained Bayesian optimization with application to aircraft design," *Aerospace Science and Technology*, Vol. 105, 2020, p. 105980.

[27] Theodorsen, T., "General theory of aerodynamic instability and the mechanism of flutter," , No. NACA Report No. 496, 1935, p. 24. https://doi.org/10.1017/CBO9781107415324.004.

[28] Murua, J., "Flexible Aircraft Dynamics with a Geometrically-Nonlinear Description of the Unsteady Aerodynamics," *PhD thesis, Imperial College London, May 2012*, 2012.

[29] Schy, A. A., and Hannah, M. E., "Prediction of jump phenomena in roll-roupled maneuvers of airplanes," *Journal of Aircraft*, Vol. 14, No. 4, 1977, pp. 375–382. https://doi.org/10.2514/3.58787, URL https://doi.org/10.2514/3.58787.

[30] Etkin, B., *Dynamics of atmospheric flight, pp. 134-145*, Dover Publications, Inc, 1972.

[31] Fang, H., Gong, C., Su, Y., H. Zhang, Li, C., and Da Ronch, A., "A gradient-based uncertainty optimization framework utilizing dimensional adaptive polynomial chaos expansion," *Struct Multidisc Optim*, 2019, pp. 1199–1219.

[32] Schmollgruber, P., "Enhancement of the conceptual aircraft design process through certification constraints management and full mission simulations," Phd thesis, Doctorat de l'Université de Toulouse délivré par l'Institut Supérieur de l'Aéronautique et de l'Espace (ISAE), Dec. 2018. URL https://hal.archives-ouvertes.fr/tel-02146110.

[33] Pedregosa, F., Varoquaux, G., Gramfort, A., Michel, V., Thirion, B., Grisel, O., Blondel, M., Prettenhofer, P., Weiss, R., Dubourg, V., Vanderplas, J., Passos, A., Cournapeau, D., Brucher, M., Perrot, M., and Duchesnay, E., "Scikit-learn: Machine Learning in Python," *Journal of Machine Learning Research*, Vol. 12, 2011, pp. 2825–2830.

[34] Cook, M. V., "Flight dynamics principles: a linear systems approach to aircraft stability and control," *Butterworth-Heinemann*, 2012.